Geomechanics and Engineering, *Vol. 36, No. 4 (2024) 367-380*
https://doi.org/10.12989/gae.2024.36.4.367

Nonlinearity effect on the dynamic behavior of the clayey basin edge

Hadi Khanbabazadeh*

Faculty of Engineering, Gebze Technical University, 41400 Gebze, Kocaeli, Turkey

(*Received October 29, 2023, Revised January 9, 2024, Accepted January 15, 2024*)

Abstract. Investigations has shown that the correct estimation of the effective amplification period is as important as the amplification value itself. It gets more important in 2D basins. This study presents a quantitative coefficient for consideration of the nonlinearity effect in terms of amplification value and the shift in its period which is missing or ineffectively considered in the previous studies. To attain this goal, by the application of a time domain fully nonlinear method, the deviation of the more common equivalent linear results from the basin nonlinear behavior under strong ground motions is investigated quantitatively. Also, despite the increase in the damping ratio, the possibility of the increase in the amplification due to the increase in motion strength is shown. To make the results useful in engineering practice, by introducing nonlinearity ratio, the effect of the nonlinearity is quantitatively estimated for two soft and stiff clayey basins with three different depths under a set of motions scaled to two target spectrum. Results show that at the 100 m depth soft clayey basin, while the nonlinearity ratio shows a 35% deviation at the basin edge part under DD1 motion level, its effect moves to the central part with 20% effect under DD3 motion level. By the increase in depth to 150 m, the results show a decrease in the overall effect of the nonlinear behavior for both clay types. At this depth, the nonlinearity ratio gives a 30% and 17% difference on a limited distance from outcrop at the soft clayey basin under DD1 and DD3 motion levels, respectively. At the 30 m depth basins, the nonlinearity ratio shows up to 25% difference for different cases. The presented ratio would be introduced as nonlinearity coefficients for consideration of the nonlinearity effects in the codes. The presented quantitative margins will help the designer to have a better understanding of the amplification period change because of nonlinearity over 2D basin surface.

Keywords: basin edge; dynamic behavior; ground motion; nonlinear behavior; numerical modeling; site effect

1. Introduction

Local site effect is influenced by several factors such as surface and subsurface topography, stratification, spatial variation of the geotechnical parameters, impedance contrast between bedrock and basin, intensity and incident angle of the incoming motions (Safak 2001). In practice, this effect is presented by the site amplification term. This term is used to show the ground motion differences between two nearby sites (Anbazhagan *et al.* 2011, Roy and Sahu 2012, Saffarian and Bagherpour 2014, Shiuly *et al.* 2015, Jakka *et al.* 2015, Zhu and Thambiratnam 2016, Pelekis *et al.* 2017, Alielahi and Adampira 2018, Mayoral *et al.* 2019). Because of the importance of the amplification factor in mitigation of earthquake damage at sedimentary sites, its precise estimation is of paramount importance.

Modeling of the wave propagation and local site effect can be done through 1D, 2D or 3D approximations. In the 1D approximation, soil layers are assumed to be extended infinitely in the horizontal direction. If the soil behavior is modeled by a proper elastoplastic model, effect of the material non-linearity can also be considered (Iyisan and Khanbabazadeh 2013, Abraham *et al.* 2015, Madiai *et al.* 2016, Griffiths *et al.* 2016, Zhu *et al.* 2018, Silahtar and Kanbur 2021). Nevertheless, its result diverges from the real behavior because of the factors such as surface and sub-surface topography as well as lateral heterogeneity. These factors give rise to reflection and refraction of body waves, wave focusing and formation of surface waves. Thus, for better estimation of the behavior, application of 2D and 3D analysis becomes necessary (Kamiyama and Satoh 2002, Makra *et al.* 2005, Makra and Chavez-Garcia 2016, Yniesta *et al.* 2017, Rodriguez *et al.* 2021). These analyses can be applied by advanced numerical methods such as finite element, finite difference, boundary element, hybrid methods, etc. (Alielahi and Adampira 2016, Kamalian *et al.* 2006, Zhang and Zhao 2009, Gelagoti *et al.* 2010, Shani *et al.* 2012, Madiai *et al.* 2017, Bordoni *et al.* 2023). Due to their cost and time consuming analyses process, presentation of the correlations between 1D and 2D/3D results are still among investigation topics (Manakou *et al.* 2010, Khanbabazadeh and Iyisan 2014a, b, Stamati *et al.* 2016, Saenz *et al.* 2019).

During an earthquake, the behavior of a sedimentary basin at time and space is the result of the interaction among incoming waves from bedrock, refracted waves at the edges as well as generated progressive surface waves. In such condition, while the resulted strains of some surface points is in elastic range, the response of some other points would reach beyond it. Also, the resonance period of the surface points can be different from each other in such conditions. As a result, a nonlinear variation of the response in time and space will happen during the history of the shaking (Sonmezer *et al.* 2018, Khanbabazadeh *et al.* 2018,

*Corresponding author, Ph.D.
E-mail: hk.babazadeh@gtu.edu.tr

ISSN: 2005-307X (Print), 2092-6219 (Online)

Table 1 Geotechnical properties of the used clay types

Soil classification		ϕ(°)	cu (kPa)	G (MPa)	K (MPa)	γ (kN/m^3)
Clay	**Soft**	10	35-45	10.1-61.2	39.1-177.3	18-20
	Stiff	10	150-165	400-900	1240-2680	20-21.5
Bedrock	**Elastic**	*	*	2200	3600	22

ϕ: internal friction angle; cu: undrained shear strength; G: shear modulus; K: bulk modulus; γ: unit weight

Stanko *et al.* 2019, Sonmezer and Celiker 2020). In this study, such behavior is referred to as the nonlinear basin response in time domain. For a reliable estimation of such response, the use of advanced nonlinear analysis method as well as proper soil constitutive model capable of considering material non-linearity is inevitable.

Although it generally becomes important for motions with PGA greater than 0.3 g, the non-linear basin response has been reported under both weak and strong motions (Wen *et al*. 2006, Nagashima *et al.* 2014). Also, some researchers have quantitatively investigated the response difference under weak and strong motions (Satoh *et al.* 1995, Field *et al.* 1997, Rong *et al.* 2016, Riga *et al.* 2018, Chandran and Anbazhagan 2020). It is known that, by the increase in the shear strain level, along with the decrease in shear modulus, damping increases. In the meantime, the resonance period of the surface points may be changed as a result of the interaction among different wave kinds. With respect to the definition of the spectral amplification factor (SAF) as the ratio of the response spectra of the surface point to the reference rock site, the general expectation is decrease in SAF by increase in the strain level. Nevertheless, greater SAF would happen due to the shift in the resonance period of a certain points. This condition would happen under both constructive and de-constructive interaction among different wave kinds at any surface points. Thus, under intense motions, the increase in damping and occurrence of the nonlinearity doesn't necessarily lead to decrease in the SAF. Also, its maximums at surface points don't occur simultaneously during the motion history (Bakir *et al.* 2002, Khanbabazadeh *et al.* 2019, Khanbabazadeh *et al.* 2020).

Finite element and finite difference methods, the boundary element method (direct and indirect methods) and hybrid techniques are among the most used numerical methods for local site effect investigations. Also, application of Meshfree Methods (MM) for modeling of the frictional contua at large displacements is also another strong technique for such inestigations (Khoshghalb *et al.* 2020, Shafee, and Khoshghalb 2021, 2022, Salehi Dezfooli *et al.* 2022). In this study, a quantitative effect of the nonlinear behavior on the basin amplification will be presented. To attain this goal, a time domain fully nonlinear method (FNM) will be applied. Unlike FNM, the widely used equivalent linear method (EQLM) uses a linear soil model along with a material degradation curve to approximate the non-linearity in the frequency domain. Although this method is simple and yields reasonable results for medium strain level, it is still an approximate method for consideration of the nonlinear dynamic soil behavior. On the other hand, any prescribed nonlinear constitutive relation can be followed in the FNM. Therefore, the effect of the variation of the shear modulus and damping ratio with strain level as well as the interaction among different waves in 2D basin can be studied in a time domain analysis (Cundall 2008). Also, through the application of an elastoplastic constitutive model with proper hardening and flow rules, more accurate estimation of the basin response is obtained (Khanbabazadeh *et al.* 2021). Nevertheless, because of the costs and difficulties of such analyses, the application of the FNM is not preferred in most cases. As a result, some of the non-linear aspects of the basin behavior affecting the amplification, including the shift in the resonance period, is neglected in EQLM analysis.

In this study, through the application of FNM and EQLM analyses, the deviation of the more common EQLM results from the FNM under strong ground motions is investigated. To make the results useful in engineering practice, dynamic response of the 2D trapezoidal clayey basins with different depths and clay types are investigated. The obtained results will presents a quantitative coefficient for consideration of the nonlinearity effect in terms of amplification value and the shift in its period which is missing or ineffectively considered in the previous studies. The presented quantitative margins will help the designer to have a better understanding of the amplification period change because of nonlinearity over 2D basin surface.

2. Basin models

Large number of the real shallow basins have got the general shape of trapezoidal with depth varying between 50 m to 150 m (Semblat *et al.* 2002, Zhu *et al.* 2018, Khanbabazadeh *et al.* 2022). Also, the underground explorations of the basins including Dinar basin (Turkey) (Khanbabazadeh *et al.* 2016), Duzce basin (Turkey) (Khanbabazadeh *et al.* 2019), French Riviera (Nice, France) (Semblat *et al.* 2000) and Gemlik basin (Turkey) (Ozaslan *et al.* 2022) have revealed the variation of the bedrock inclination at the basin edge between 5º to 20º. In the smaller bedrock inclinations, greater basin surface is affected by the basin edge (Iyisan and Khanbabazadeh 2013, Khanbabazadeh and Iyisan 2014a). Based on these data, and to make the results useful in practical engineering works, three different shallow trapezoidal basins with 30 m, 100 m and 150 m depths, and bedrock inclination of 10º have been selected, as shown in Fig. 1. Since the basin edge effect exceeds beyond the horizontal projection of the inclined bedrock at the surface, the width of the basins has been taken so long that the whole edge effect could be seen

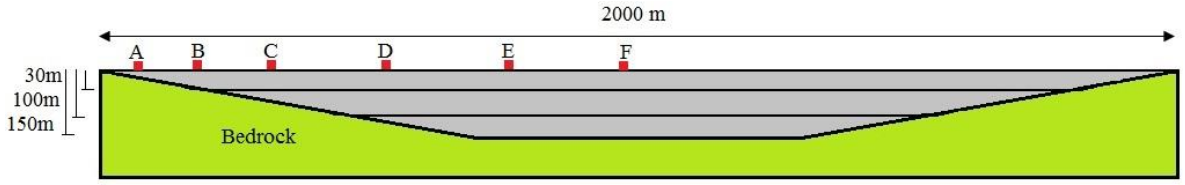

Fig. 1 Geometry of the 2D shallow clayey basins with different depths and recording surface points

(2 km). The sufficiency of this selection has been checked out by several test analyses. During the fully non-linear analyses, the acceleration time history at the basin surface is recorded. The location of the recorded surface points is shown in Fig. 1.

To see the effect of the clay type, two types of the soft and stiff clays are considered. Their geotechnical properties are presented in Table 1. To reflect the field condition, a linear variation of the geotechnical specifications over basin depth has been considered. The values in the Table 1 are for variation over 100 m. The proportional values have been assigned for other depths beginning with similar values at the surface.

3. Earthquake motions

The considered sedimentary basin models are subjected to a collection of twenty-four earthquakes scaled to two different strength levels of DD1 and DD3 with respect to Turkish seismic code provisions. The probability of exceedance of DD1 and DD3 levels in 50 years are 2% (with a return period of 2475 years) and 50% (with a return period of 72 years), respectively. The target spectra corresponding to DD1 and DD3 motion levels are presented in Fig. 2. The applied earthquake motions have been selected from among motions recorded during real earthquakes with different frequency contents and durations. All of them have been recorded on rock or rock-type layer with shear wave velocity greater than 750 m/s, or de-convoluted to the corresponding bedrock motion. The used records are baseline corrected and filtered by 20 Hz low-pass filter. Therefore, each model is analyzed by two FNM and EQLM methods under a collection of twenty-four motions with two strength levels. The specifications of the used strong ground motion set are presented in Table 2.

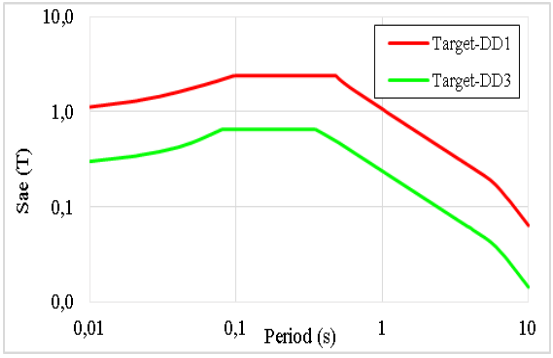

Fig. 2 Target spectra corresponding to target DD1 and DD3 motion levels (ξ=5%)

4. Analysis method

4.1 Fully nonlinear analysis method

Although the EQLM is the common method in the literature due to its simplicity, it cannot capture the non-linear aspects of the basin behavior properly. The applied FNM is based on explicit finite difference scheme to solve full equations of motion using lumped grid-point masses derived from the real density of surrounding zones. Its application range covers large strain level. Due to the flexibility of the finite difference method in the modeling of the irregular geometries and nonlinear behavior of soils, this method has been chosen for the present set of analyses. The codes of the modeled basins are performed inside FLAC3D environment. A brief explanation of the method by emphasize on the plasticity/non-linearity features is be presented. Constant strain-rate tetrahedra elements have been used for the molding of the continuum. These elements have the advantage of not generating hourglass deformations. To overcome overly stiff response, a process of mixed discretization is applied to give the element more volumetric flexibility by proper adjustment of the first invariant of the tetrahedra strain-rate tensor. Through the increase in the discretization efficiency, better estimation of the modeling of the reflected and refracted waves from irregularities with different geometries are achieved. To prevent the numerical distortion of the dynamic analysis, based on Kuhlemeyer and Lysmer (1973), the spatial element size was applied smaller than one tenth to one eighth of the wavelength associated with the highest frequency component of the applied wave. For the present study, the mesh dimension is considered as 1m. An elastoplastic nonlinear constitutive relation has been used in the FNM. It is characterized by its yield function, hardening functions and flow rule. The failure envelope corresponds to a Mohr-Coulomb criterion (shear yield function) with tension cutoff (tension yield function). The position of a stress point on the envelope is controlled by a non-associated flow rule for shear failure, and an associated rule for tension failure. Because of its capability in the reproduction of the irreversible strain accumulation during seismic loading, a better estimation of the non-linearity can be obtained. The shear modulus reduction curve (G/G_{max}) is also defined inside the behavior model formulation using special built-in function forms. The utilized shear modulus reduction curves are presented in Fig. 3.

4.2 Damping

Because of their simplicity in application, the local,

Table 2 Specifications of the used strong ground motions

	Earthquakes	Station	Amax (g)	Magnitude	R_{JB}	Arias Intensity (m/s)
1	Tottori_ Japan(10.06.2000)	OKYH07	0.1	Mw=6.61	15.23	0.3
2	Kocaeli_Turkey (17.08.1999)	Gebze	0.1	Mw=7.51	7.57	0.5
3	Mammoth lakes (25.05.1980)	USC McGee Creek	0.1	Mw=6.0	6.68	0.1
4	Anza (25.02.1980)	PinyonFlat	0.1	Mw=5.19	12.24	0.0218
5	Palm springs1986	Silent Valley	0.1	ML=5.9	19.5	0.1
6	Chalfant (21.07.1986)	LongValleyDam	0.1	Mw=6.2	14.97	0.2
7	Sakarya (11.11.1999)	Development burea	0.2	Md=5.7	17.5	0.1397
8	Dinar (01.10.1995)	Dinar station	0.2	ML=5	2	0.8096
9	Duzce (12.11.1999)	Lamont-531	0.2	Mw=7.1	11.4	0.5283
10	Cape Mendocino (RSN-3744) (1992)	Bunker Hill FAA	0.2	Mw=7.01	8.49	0.6
11	Tottori_ Japan(10.06.2000	SMNH10	0.2	Mw=6.61	15.58	0.5
12	Parkfield-02_ CA(28.09.2004)	Turkey Flat#1(0M)	0.2	Mw=6	4.66	0.2
13	Mendocino 1992	EEL River valley	0.3	ML=6.5	15	0.8079
14	Coyotelake (06.08.1979)	Coyote Lake Dam	0.3	Mw=5.7	1.6	0.4003
15	Parkfield (28.06.1966)	Temblor pre	0.3	Mw=6.1	16.1	0.3615
16	Firuzabad 20.06.1994	Firuzabad-ZRT	0.3	Mw=5.9	21	0.687
17	Kobe_ Japan(16.01.1995)	Kobe University	0.3	Mw=6.9	0.9	1.2
18	Hector Mine(16.10.1999)	Hector	0.3	Mw=7.13	10.35	1.9
19	Kocaeli1 (RSN-1165) (07.08.1999)	Izmit	0.4	Mw=7.51	3.62	0.8
20	Parkfield (28.06.1996)	Temblorpre	0.4	Mw=6.1	16.1	0.5537
21	UmbriaMarche (10.16.1997)	Colfiorito-Casermette	0.4	Mw=4.3	1	0.6902
22	South Iceland (17.06.2000)	Thjorsarbru	0.4	Mw=6.5	15	1.6125
23	Manjil_Iran(20.06.1990)	Abbar	0.4	Mw=7.37	12.55	7.5
24	RSN9071-AZPFOHL(12.06.2005)	Pinon Flats Observatory	0.4	Mw=5.2	12.82	0.3

artificial viscosity and Rayleigh damping are among the widely used schemes in common dynamic analyses. Nevertheless, the frequency independency of the soil damping isn't correctly considered in them. To overcome this short-coming, a frequency independent hysteresis damping is implemented in this study. Unlike the equivalent linear method that uses predefined damping curve, the applied finite differences based fully nonlinear method uses a proper elastoplastic constitutive relation so that the plasticity formulation relates plastic strain increments to the stresses. The formulation of the hysteresis damping is implemented by modifying the strain-rate calculation. In this scheme, by the definition of the modulus reduction curve (Fig. 3) for each soil type through the built-in special functions, the fitting process is fulfilled by an iterative adjustment of the curves for each point using a separate FLAC code. During the analysis, the scheme is implemented by modifying the strain-rate calculation so that the mean strain-rate tensor (averaged over all subzones) is estimated before application of the constitutive model functions. On the other hand, the used elatoplastic relation has a constant, tangent, elastic shear modulus, G_{max}, and yield shear stress, τ_m._By the application of the hysteretic damping with an elastoplastic model, the combination of the Hardin/Drnevich hysteretic damping with a Mohr-Coulomb model is utilized. In this condition, the yield level of the hyperbolic law should be greater than the Mohr-Coulomb yield shear stress.

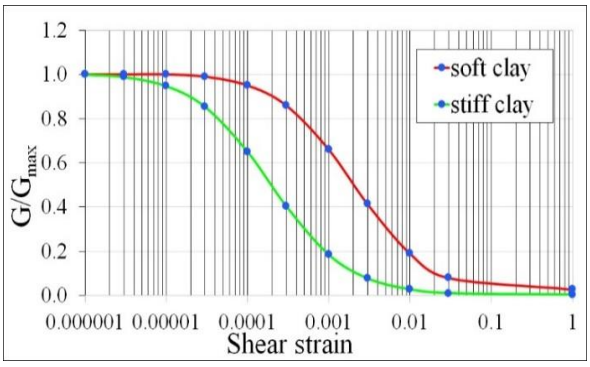

Fig. 3 Modulus reduction curves of the studied clay materials

4.2 Damping

Because of their simplicity in application, the local, artificial viscosity and Rayleigh damping are among the widely used schemes in common dynamic analyses. Nevertheless, the frequency independency of the soil damping isn't correctly considered in them. To overcome this short-coming, a frequency independent hysteresis damping is implemented in this study. Unlike the equivalent linear method that uses predefined damping curve, the applied finite differences based fully nonlinear method uses a proper elastoplastic constitutive relation so that the plasticity formulation relates plastic strain increments to the

stresses. The formulation of the hysteresis damping is implemented by modifying the strain-rate calculation. In this scheme, by the definition of the modulus reduction curve (Fig. 3) for each soil type through the built-in special functions, the fitting process is fulfilled by an iterative adjustment of the curves for each point using a separate FLAC code. During the analysis, the scheme is implemented by modifying the strain-rate calculation so that the mean strain-rate tensor (averaged over all subzones) is estimated before application of the constitutive model functions. On the other hand, the used elatoplastic relation has a constant, tangent, elastic shear modulus, G_{max}, and yield shear stress, τ_m._By the application of the hysteretic damping with an elastoplastic model, the combination of the Hardin/Drnevich hysteretic damping with a Mohr-Coulomb model is utilized. In this condition, the yield level of the hyperbolic law should be greater than the Mohr-Coulomb yield shear stress.

4.3 Boundary condition

Two different boundary conditions have been applied to the horizontal and vertical boundaries. To consider the condition of the incoming wave, compliant base boundary scheme has been applied in the model base. Also, a transition layer has been defined between the bottom boundary and the basin material. In this way, in addition to the propagation of the incoming waves into the model, the reflected waves inside the model will exit from this boundary (Lysmer and Kuhlemeyer 1969). The vertical boundaries at the model sides have been located 100 m away from the basin edge. In addition to that, free-field boundary condition has been utilized. During the dynamic analysis, the free-field calculations is executed in parallel with the main-grid analysis. The effectiveness of this scheme to absorb body waves approaching at incidence angles greater than 30° has been widely approved (Cundall 1980). Besides, the results of several test analyses showed the sufficiency of the vertical boundary distance at the sides. Fig. 4 shows the schematic connection of the main grid to the applied boundary conditions.

4.4 Equivalent linear method

FNM needs more user involvement as well as very long analysis time especially for models under real earthquake motions. For these reasons, EQLM is widely used as one of the alternative methods in geotechnical earthquake engineering. In this analysis method, a shear modulus reduction coefficient and damping ratio is defined as a function of effective strains. An iterative calculation is repeated until strain compatible stiffness and damping ratio are obtained at all elements. The equivalent linear analyses of this study are performed by SuperFLUSH (1995) which is a 2D strain dependent finite element program in frequency domain. It is based on the assumption of plane strain condition and also considers the energy dissipation in and out-of-plane directions. The material properties and dynamic motions used for the FNM analyses will be used for the ELM models.

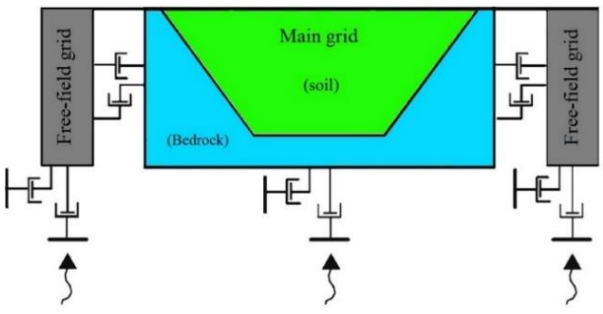

Fig. 4 Schematic coupling of the main grid to free-field grids and quiet boundary viscous dashpots

4.5 Verification

To verify the applied numerical modeling, the response of a trapezoidal basin estimated by Zhu and Thambiratnam (2016) subjected to the Ricker pulse has been used. The specification of the applied Ricker pulse as well as the basin geometry have been presented in Fig. 5. The variation of the basin surface displacement with time is presented for both modeled and reference solutions in Fig. 6. The closeness of the results is good.

5. Results and discussion

Since the main goal of this study is to present a quantitative effect of the nonlinearity on the basin dynamic behavior, firstly the increase in the amplification due to the increase in motion strength due to the shift in the resonance period will be investigated for two example motions. Then, the comparison between the spectral amplification factors of the clayey basins estimated by FNM and EQLM will be presented. Finally, the nonlinearity ratio, which is defined as the ratio of the maximum spectral amplification (MSAF) estimated by FNM to EQLM at each surface point averaged for the twenty-four motion set, will be presented for three different basin depths at two motion levels of DD1 and DD3.

5.1 Nonlinear basin behavior effect on spectral amplification

In this section, the results of the time domain fully nonlinear analyses of the 100m depth basin subjected to two certain earthquake motions are investigated. Figs. 7 and 8 show the acceleration response spectra at the surface points of the soft clayey basin with 100 m depth subjected to the motion No.10 (RNS 3744) (Table 2) scalded to DD3 and DD1, respectively. Also, for comparison, the response spectrum of the free-field scaled to the same strength levels has been presented. Comparing Figs. 7 and 8 shows that while under weaker DD3 motion level the maximum response at all surface points are at period smaller than the free-field motion, it exceeds the free-field maximum response period at points C and D under stronger DD1 motion level.

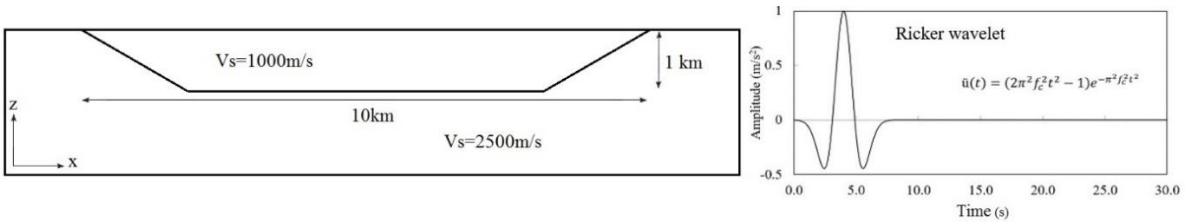

Fig. 5 Specification of the used basin geometry and the applied Ricker pulse for verification

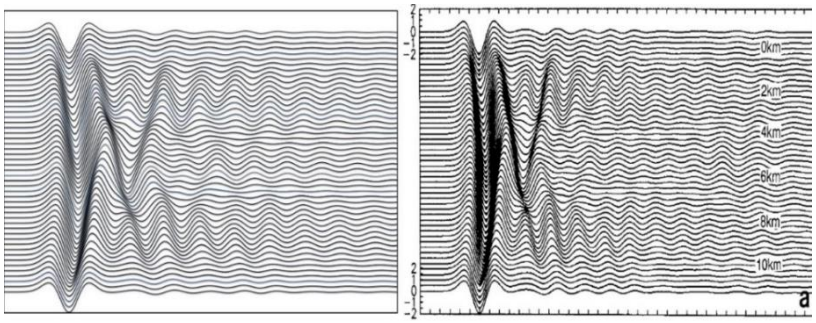

Fig. 6 Comparison of the results of the verification model and the present study

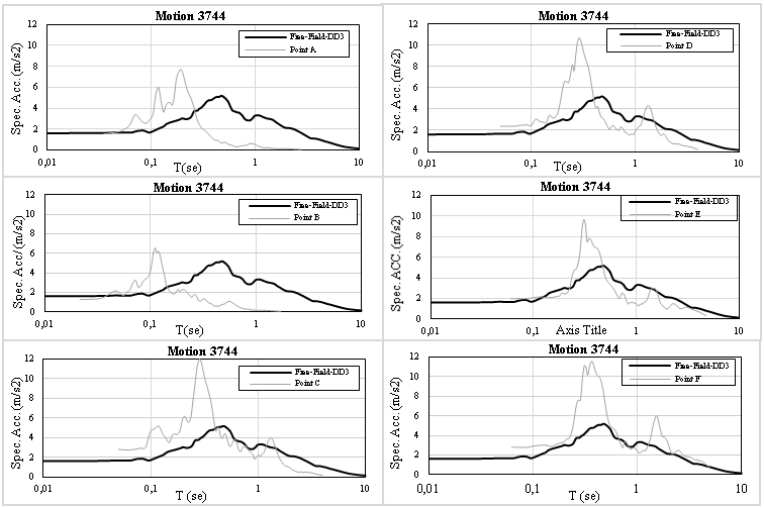

Fig. 7 Acceleration response spectra at the surface points subjected to the motion No.10 (RNS 3744) scaled to DD3 level

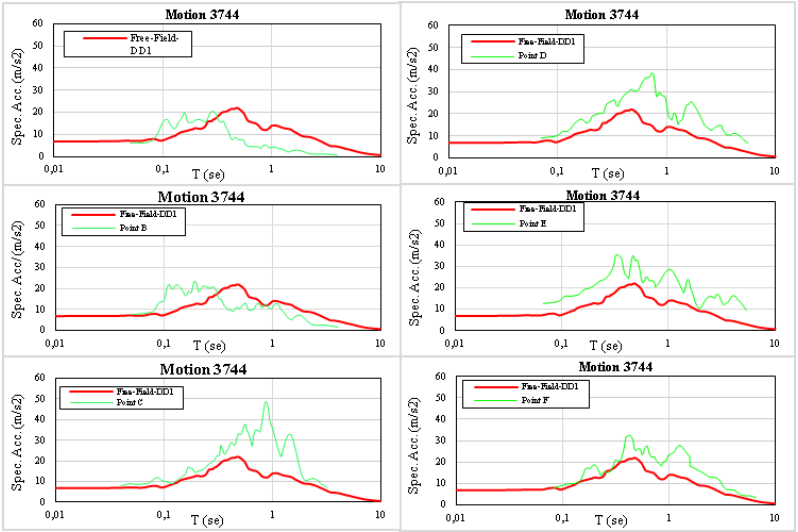

Fig. 8 Acceleration response spectra at the surface points subjected to the motion No.10 (RNS 3744) scaled to DD1 level

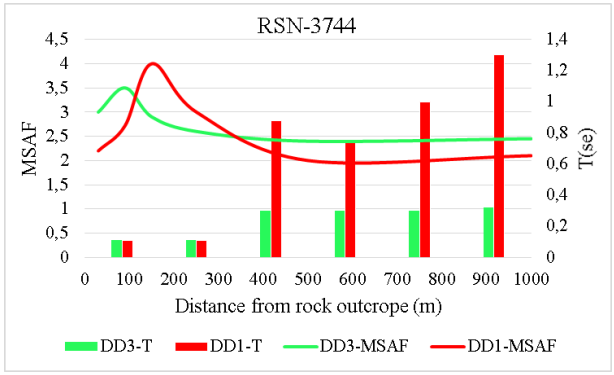

Fig. 9 Variation of the MSAF and their corresponding period at each surface point under motion No.10 (RNS 3744) scaled to DD3 and DD1 motion levels

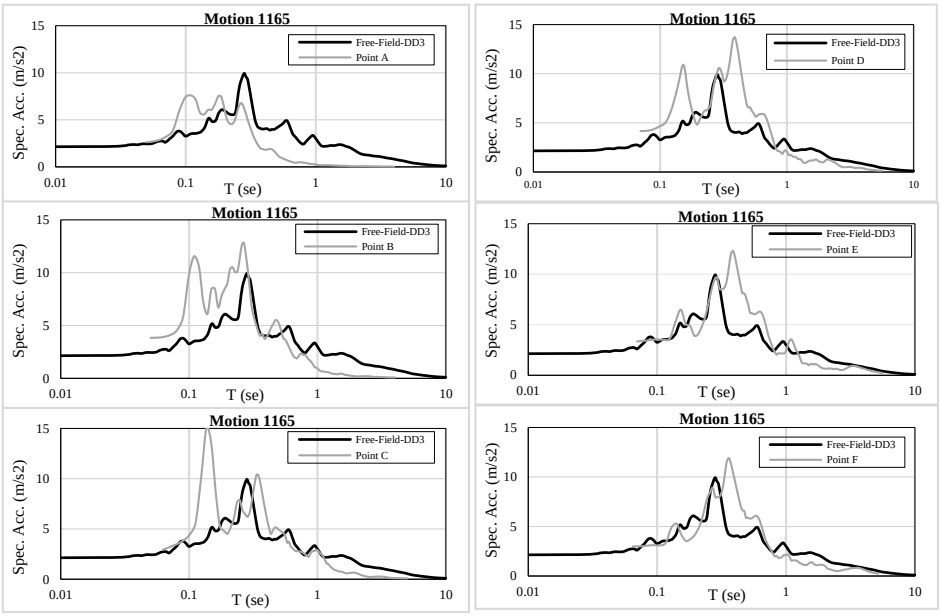

Fig. 10 Acceleration response spectra at the surface points subjected to the motion No.19 (RNS 1165) scaled to DD3 level

The system Defining SAF as the ratio of the spectral acceleration at each surface point to the free-field at corresponding period, the effect of the nonlinearity on the variation of the maximum SAF (MSAF) can be investigated in more detail. Fig. 9 shows the variation of the MSAF and their corresponding period at each surface point under motion RNS-3744 scaled to DD3 and DD1 motion levels. As can be seen, the corresponding period of the MSAF at points A and B is almost the same but with greater MSAF value under DD3 motion level. At points C and D, the MSAF under DD1 level happens at greater period with respect to DD3. Comparing the response spectrum of these two points with respect to the free-field at Fig. 8 shows the smaller spectral value of the free-field at the period used for estimation of MSAF. At points E and F, despite the shift in the period of their maximum spectral values, the resulted MSAF under DD1 level is smaller than DD3.

This effect is investigated for another bedrock motion. Figs. 10 and 11 show the acceleration response spectra of the surface points estimated by FNM in time domain subjected to No. 19 motion (RNS 1165) scalded to DD3 and DD1, respectively. For this motion, the noticeable shift in the resonance period because of the change in motion strength has happened at point C. For more insight, the variation of the MSAF and corresponding period at surface points have been presented in Fig. 12 shows. Despite almost close resonance period under both DD3 and DD1 levels at point D, the resulted MSAF under stronger DD1 level is greater than DD3 one. Also, despite the shift in the period at point C, the resulted MSAF at DD1 is smaller than DD3. Such behaviors can be seen in the results of the time domain FNM analyses. It should be mentioned that the above seen conditions doesn't necessarily happen under all earthquakes, but it shows that under stronger motions, despite the increase in the shear strain level and resulted greater damping, greater MSAF can be resulted because of the shift in the period of the maximum spectral value at certain surface points.

To see the difference between basin nonlinear behavior and the behavior estimated by the traditional EQLM, the amplification behavior of the basin estimated by two methods under preceding two example motions have been

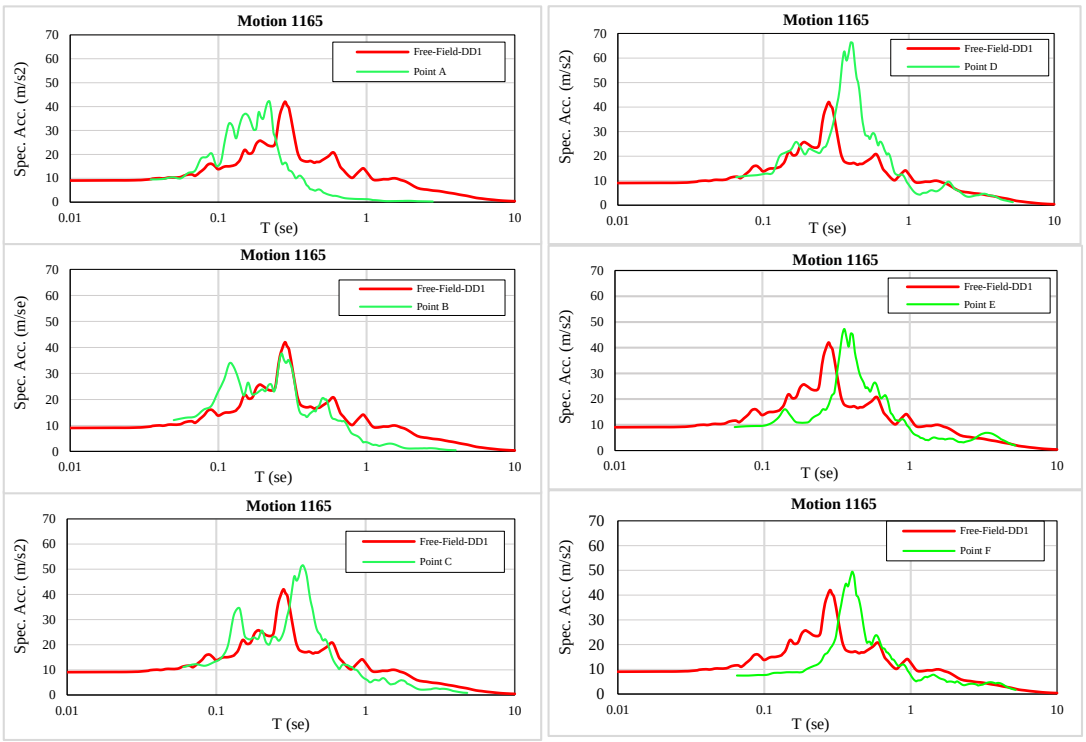

Fig. 11 Acceleration response spectra at the surface points subjected to the motion No.19 (RNS 1165) scaled to DD1 level

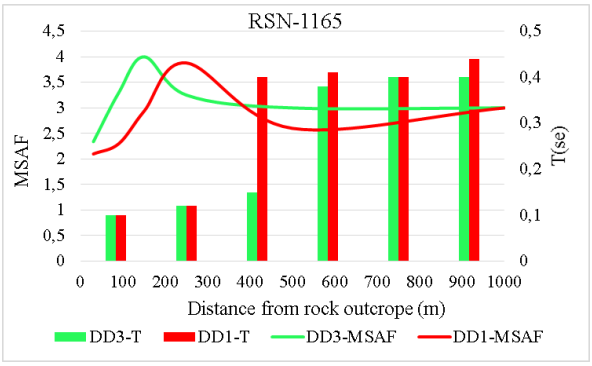

Fig. 12 Variation of the MSAF and their corresponding period at each surface point under motion No.19 (RNS 1165) scaled to DD3 and DD1 motion levels

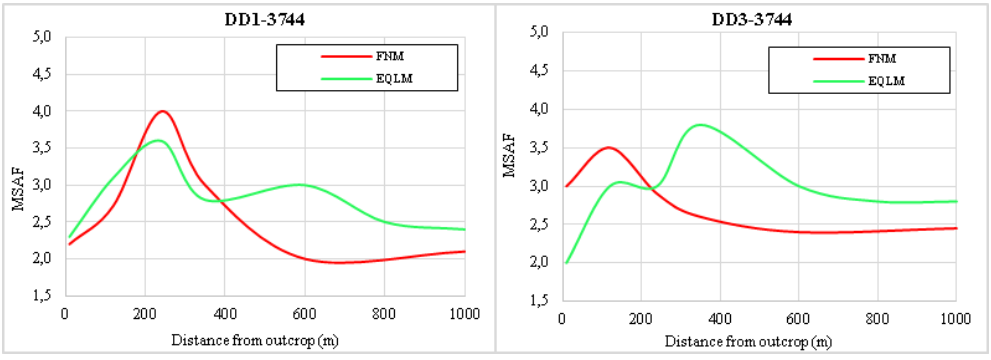

Fig. 13 Comparison between FNM and EQLM results under motion No.10 (RNS 3744)

presented in Figs. 13 and 14. Fig. 13 shows that, for motion RSN-3744, although the estimated MSAF by the EQLM at DD3 level is greater than FNM over most of the basin surface, the location of the maximum value is different. For DD1 level, despite the close amplification trend at the basin edge area, greater MASF has been estimated by the FNM. For this case, the results of the EQLM is greater beyond the 400 m from the outcrop. Also, by the increase in the motion

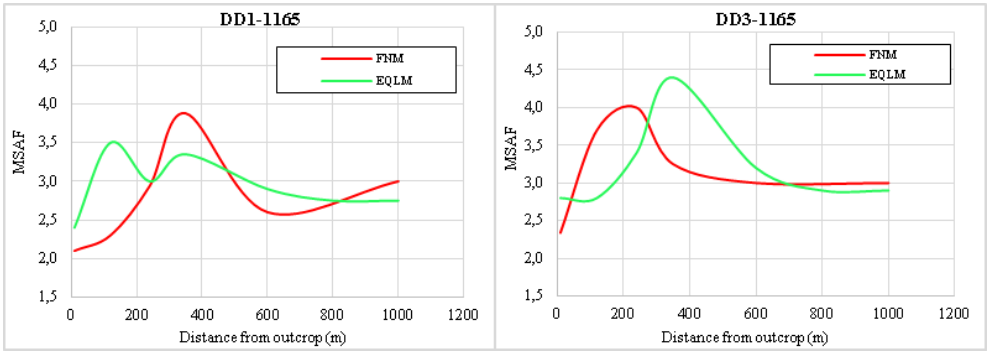

Fig. 14 Comparison between FNM and EQLM results under motion No.19 (RNS 1165)

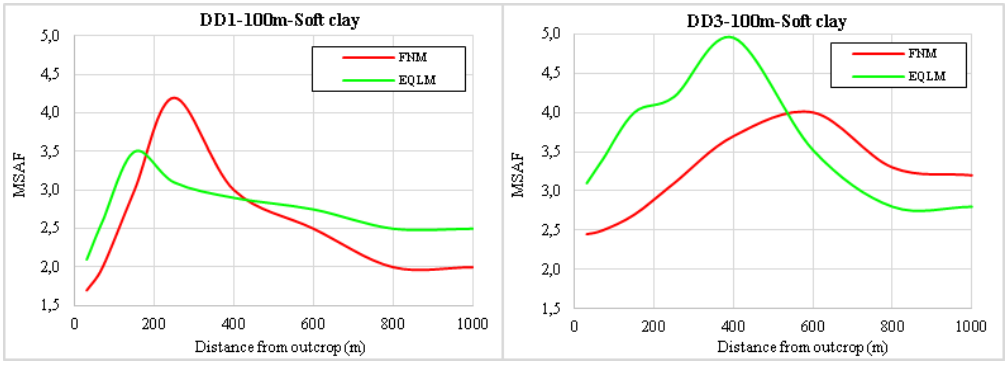

Fig. 15 Behavior of the soft clayey basin (100 m depth) under two motion strength levels

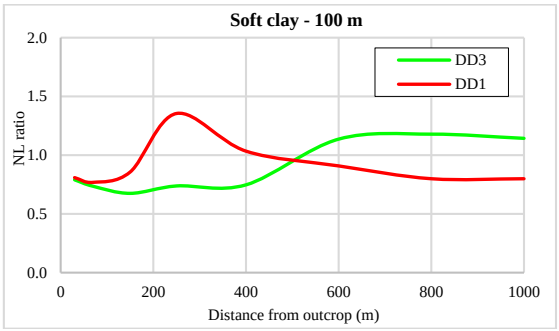

Fig. 16 Variation of the nonlinearity ratio at the soft clayey basin (100 m depth) under two strength levels

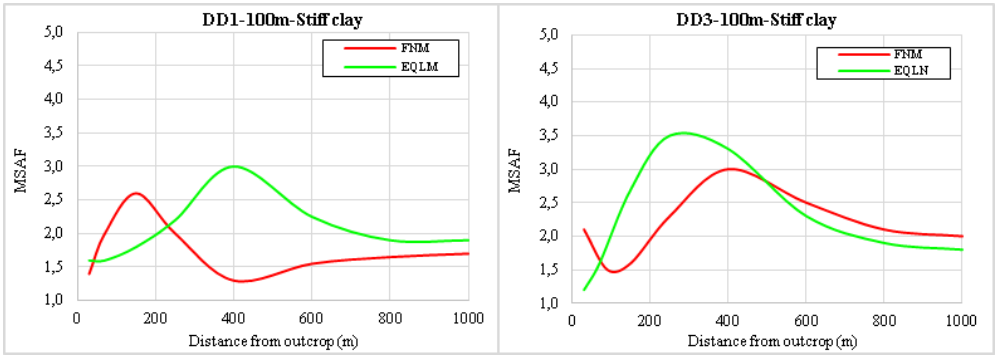

Fig. 17 Behavior of the stiff clayey basin (100m depth) under two motion strength levels

strength from DD3 to DD1, while the maximum MSAF estimated by EQLM has been decreased from 3.85 to 3.55, the FNM have resulted in an increase from 3.5 to 4.

For the RSN-1165 motion case (Fig. 14), the value and location of the maximum MSAF estimated by EQLM are different from FNM result for DD3 level. By the increase in the motion strength to DD1 level, the maximum MSAF value of the FNM becomes greater than EQLM. Also,

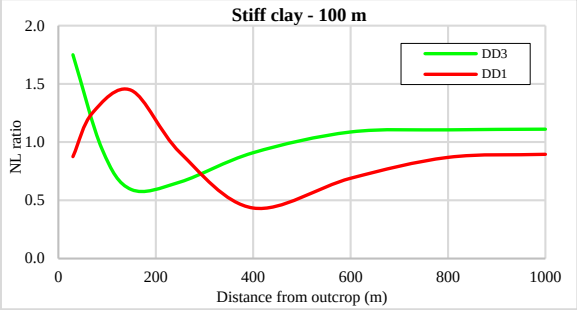

Fig. 18 Variation of the nonlinearity ratio at the stiff clayey basin (100 m depth) under two strength levels

despite the decrease in the maximum MSAF estimated by EQLM from 4.4 to 3.5, almost the same value has been resulted in by the FNM.

5.2 Nonlinearity effect on MSAF in clayey basins

In the following sections, the difference of the nonlinear basin behavior from traditional EQLM estimations will be presented quantitatively. To remove the result dependency to certain motion, the averaged basin amplification response to twenty-four earthquake motions will be presented. To this end, the considered trapezoidal basins with different depths and clay types are analyzed by a set of strong ground motions scaled to DD1 and DD3 strength levels.

5.2.1 Effect of the clay type

Fig. 15 shows the behavior of the soft clayey basin with 100 m depth under two motion strength levels. It is seen that at the DD3 level the results of the EQLM method are dominant at the edge area. For this case, the maximum difference reaches to 35% at 400 m from the outcrop. At the DD1 level, although the EQLM results are dominant at most of the basin surface, the maximum MSAF has been resulted in at 250 m from the outcrop with 0.35% difference by FNM.

To see the difference better, Fig. 16 shows the nonlinearity ratio as the ratio of MSAF estimated by FNM to EQLM averaged for twenty-four motions for two motion levels of DD1 and DD3. It is seen that under DD1 motions the ratio is greater than 1between 200 m and 400 m at the basin edge where the interaction among different wave kinds is more critical. At the weaker DD3 level, the FNM results are dominant beyond 500 m from the outcrop.

At the stiff clayey basin, Fig. 17 shows that at DD3 level there is a proximity between the results of both methods beyond about 500 m from the outcrop. Nevertheless, EQLM results are dominant at edge part. By the increase in the motion strength level, EQLM yields greater values at area beyond about 200 m from the outcrop, while FNM results are greater at the critical area close to outcrop.

At the stiff clayey basin, the nonlinearity ratio greater than unity, shown in Fig. 18, indicates the domination of the nonlinear behavior at the basin edge area at DD1 level. Also, nonlinearity ratio of about 1 beyond 400 m from the outcrop shows the absence of nonlinearity at this area at DD3 level.

5.2.2 Depth effect on nonlinear behavior

5.2.2.1 Basins with 30 m depth

Fig. 19 shows the behavior of the shallowest basin of this study with soft and stiff clayey soils. At the soft clayey basin, beyond almost 250 m from the outcrop the nonlinear behavior is dominant under both motion levels. It can be related to the sensitivity of middle part of the shallow basins to longer periods with larger particle motion level. The condition gets reverse for the 30m depth stiff clayey basins. Except at short distance from the outcrop, the results of EQLM is greater indicating the conservative results of EQLM at shallow stiff basins.

Fig. 20 shows that the nonlinearity ratio in the soft clayey basin is greater than unity beyond almost 250 m from the outcrop indicating the nonlinear behavior in this part under both motion strength levels. On the other hand, it is smaller than unity beyond 200 m from the outcrop in the stiff clayey basin indicating no nonlinear behavior in this part. Under the DD1motion level, the results of the FNM is dominant at 200 m from the outcrop in the stiff clayey basin.

5.2.2.2. Basins with 150 m depth

Fig. 21 shows that the soft clayey basin surface with 150 m depth can be divided into three parts with respect to its behavior. The FNM results are dominant at the middle part under both strength levels. It can be related to the effect of the progressive surface waves that can be considered by the time domain FNM method. The trend seen in the 150m depth stiff clayey basin is to some extent similar to the behavior of the 30 depth stiff clayey basin but with smaller MSAF values. Except in the short part close to the outcrop under DD1 strength level, the result of the EQLM is conservative for whole basin surface. Considering the stiff clayey basins with different depths, it can be concluded that the EQLM results are conservative under both motion strength levels.

Considering the greater horizontal projection of the inclined bedrock at the basin surface with 150 m depth, the variation of the nonlinearity ratio in Fig. 22 shows that in the soft clayey basin it is greater than unity for both motion strength levels between roughly 300 m and 600. In this part, while the deviation from FNM results is about +20% under DD3 level, it reaches to about +45% under DD1 level. For the Stiff clayey basin, the nonlinearity ratio is less than unity under DD3 level indicating the conservative results of

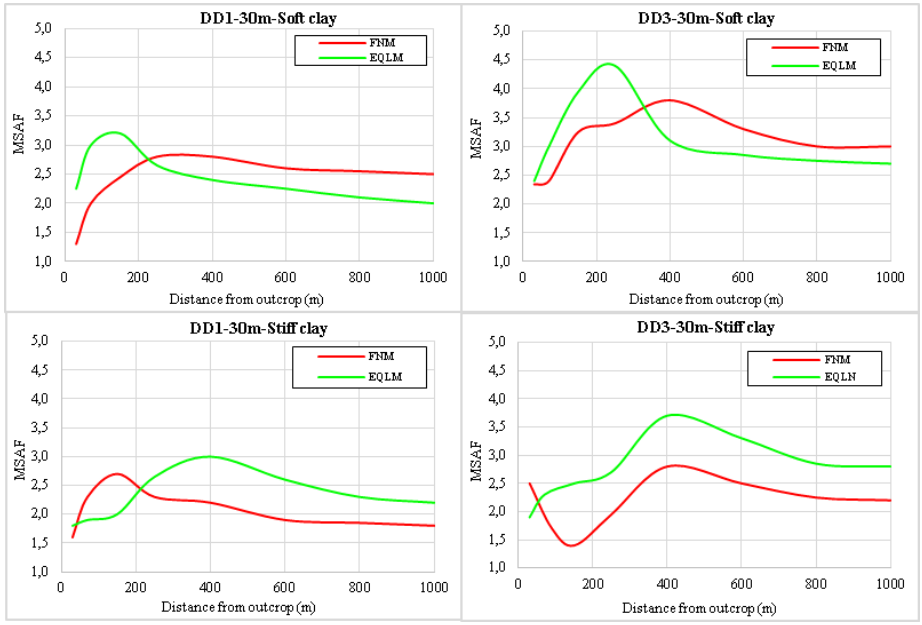

Fig. 19 Behavior of the soft and stiff clayey basins (30 m depth) under two motion strength levels

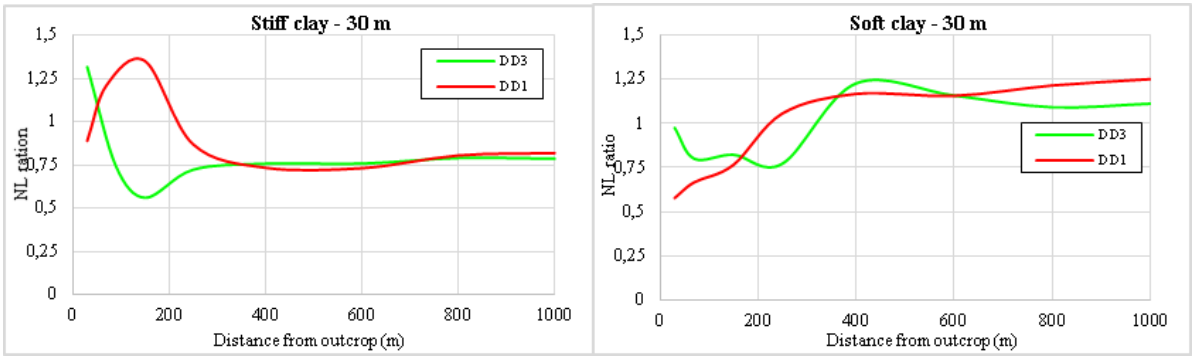

Fig. 20 Variation of the nonlinearity ratio at the soft and stiff clayey basins (30 m depth) under two motion strength levels

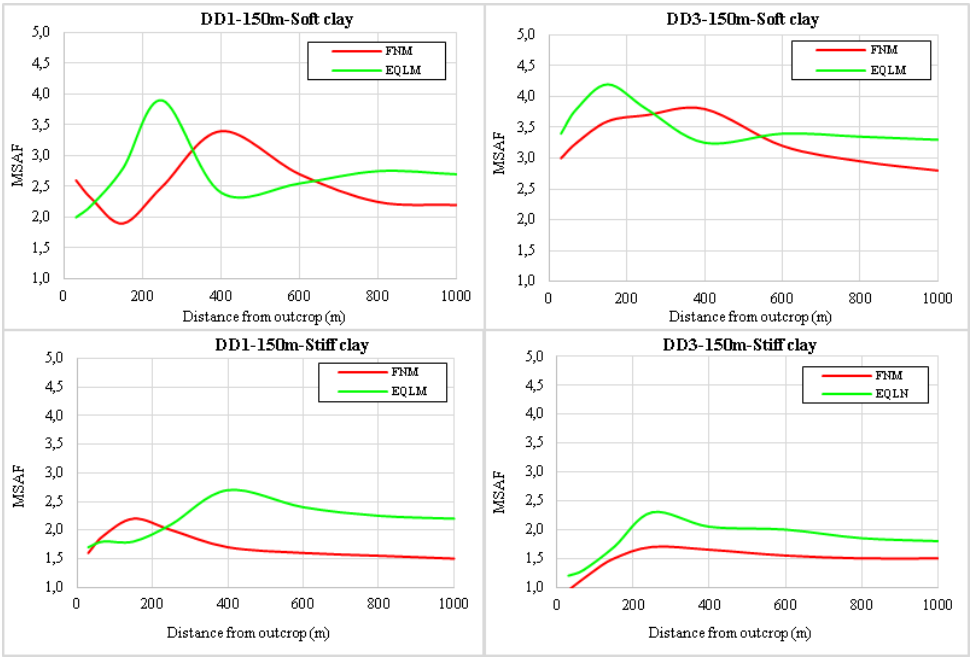

Fig. 21 Behavior of the soft and stiff clayey basins (150 m depth) under two motion strength levels

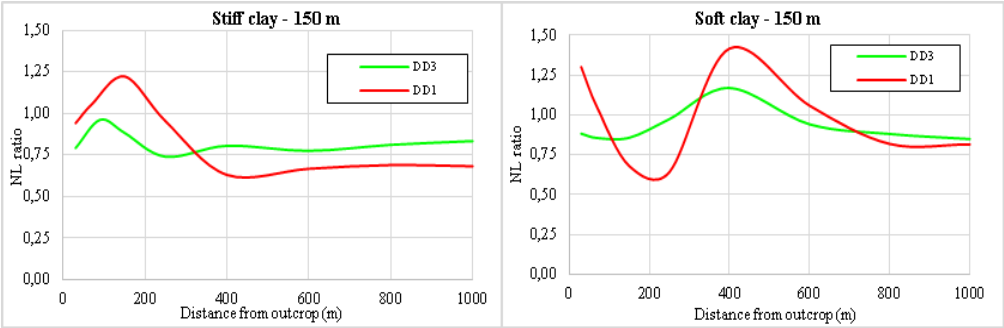

Fig. 22 Variation of the nonlinearity ratio at the soft and stiff clayey basins (150 m depth) under two motion strength levels

the EQLM for 150 depths. Under DD1 level, while the EQLM results are conservative for the basin surface beyond about 250 m from the outcrop, the deviation from FNM results reach up to 25% in the basin edge part.

The nonlinear dynamic behavior of the 2D basins are affected by different parameters such as geotechnical parameters, basin geometry as well as the specifications of the applied numeric method. The results of this study is applicable only for clayey basins with more frequently encountered bedrock inclination of 10°. Independent investigations must be applied for other basins such as sandy basins or basin with different bedrock inclination at the basin edges.

Deterministic local site effect investigation is based on the general response of the continua. The effect of the parameters such as saturation, void ratio etc. are generally reflected in the material specification such as shear wave velocity, damping and modulus reduction curves. It needs an independent wide parametric dynamic analysis to show such effects on the basin response. Nevertheless, the results of this study can be used for any clayey soil with saturation and void ratio combinations that results in shear wave velocity of the used soil types.

6. Conclusions

During motion history, interaction among different wave kinds results in different strain levels along basin surface leading to possible shift in the resonance period. Despite greater damping ratio, it would cause greater spectral amplification under stronger motions with respect to the weaker motions. In this study, by the application of a time domain fully nonlinear method, the deviation of the more common EQLM results from the basin nonlinear behavior under strong ground motions was investigated.

- Firstly, through the detailed investigation of the basin behavior under two example motions, it was shown that the increase in the motion strength doesn't necessarily yields smaller spectral amplification. Then, by introducing nonlinearity ratio, the effect of the nonlinear basin behavior on spectral amplification was quantitatively presented for two soft and stiff clayey basins with three different depths. To remove the motion dependency, and to make the results useful in engineering practice, the nonlinearity ratio of each basin was estimated as the average of twenty-four earthquake motions.
- At the 100 m depth soft clayey basin, the results show a 20% effect of the nonlinearity on the maximum response under DD1 level, while an overestimated value has been yield by EQLM under DD3 level. The estimated nonlinearity ratio indicates a 35% deviation from FNM results under DD1 level between 200 m and 400 m at the edge. Under DD3 level an almost constant 20% difference has been estimated for basin middle part. At the 100 m depth stiff clayey basin, except at the limited 200 m edge part under DD1 level, no nonlinear effect was seen.
- By the increase in the basin depth to 150m the overall effect of the nonlinear behavior decreases. The maximum response of the soft clayey basin estimated by FNM is smaller under both motion levels. Apart from maximum response, the nonlinearity ratio showed a 30% and 17% difference just between 300 m and 500 m from the outcrop under DD1 and DD3 motion levels, respectively. At the stiff clayey basins, the EQLM results are almost dominant at whole basin surface. The nonlinearity ratio is smaller than unity at almost all points under both motion levels. Such behavior of the deeper basin can be related to the smaller effect of the basin edge and nonlinear effect at deeper basins.
- The results showed that just the central part of the soft clayey basin with 30m depth is affected by the nonlinear behavior under both motion levels. With respect to the nonlinearity ratio, it remains under 25%. Regarding the shallow stiff clayey basin, while no nonlinearity is seen under DD3 level with ratio less than 1, there is an about 20% nonlinearity effect at the edge part under DD1 level.
- Based on the results of this study, it can be concluded that under DD1 level a 20% increase in the maximum response will give a reliable estimation of the nonlinearity at the soft clayey basin. Although the maximum response of the other basins estimated by EQLM are overestimated, it doesn't mean the absence of the nonlinearity at other parts. To consider the nonlinear behavior effect at these parts, the EQLM results can be increased up to 30%.
- The results of this study is applicable for clayey basins. Also, the present study has been done for more frequently encountered bedrock inclination of 10°. Independent investigations must be applied for other basins such as sandy basins or basin with different bedrock inclination at the basin edges.

References

Abraham, J.R., Lai, C.G. and Papageorgiou, A. (2015), "Basin-effects observed during the 2012 Emilia earthquake sequence in Northern Italy", *Soil Dyn. Earthq. Eng.*, **78**, 230-242. https://doi.org/10.1016/j.soildyn.2015.08.007.

Alielahi, H. and Adampira, M. (2016), "Site-specific response spectra for seismic motions in half-plane with shallow cavities", *Soil Dyn. Earthq. Eng.*, **80**, 163-167. https://doi.org/10.1016/j.soildyn.2015.10.003.

Alielahi, H. and Adampira, M. (2018), "Evaluation of 2D seismic site response due to hill-cavity interaction using boundary element technique", *J. Earthq. Eng.*, **22**(6), 1137-1167. https://doi.org/10.1080/13632469.2016.1277437.

Anbazhagan, P., Aditya, P. and Rashmi, H.N. (2011), "Amplification based on shear wave velocity for seismic zonation: comparison of empirical relations and site response results for shallow engineering bedrock sites", *Geomech. Eng.*, **3**(3), 189-206. https://doi.org/10.12989/gae.2011.3.3.189.

Bakir, B.S., Ozkan, M.Y. and Ciliz, S. (2002), "Effects of basin edge on the distribution of damage in 1995 Dinar, Turkey earthquake", *Soil Dyn. Earthq. Eng.*, **22**, 335-345. https://doi.org/10.1016/S0267-7261(02)00015-5.

Bordoni, P., Gori, S., Akinci, A., Visini, F., Sgobba, S., Pacor, F., Cara, F., Pampanin, S., Milana, G. and Doglioni, C. (2023), "A site-specific earthquake ground response analysis using a fault-based approach and nonlinear modeling: The case pente site (Sulmona, Italy)", *Eng. Geol.*, **314**, 106970, https://doi.org/10.1016/j.enggeo.2022.106970.

Chandran, D. and Anbazhagan, P. (2020), "2D nonlinear site response analysis of typical stiff and soft soil sites at shallow bedrock region with low to medium seismicity", *J. Appl. Geophys.*, **179**, 104087, https://doi.org/10.1016/j.jappgeo.2020.104087..

Cundall P.A. *et al.* (1980), *NESSI—soil structure interaction program for dynamic and static problems*. Norwegian Geotechnical Institute, Report 51508-9.

Cundall, P.A. (2008), *FLAC3D Manual: a computer program for fast Lagrangian analysis of Continua (Version 4.0)*. Minneapolis, MN, USA.

Field, E.H., Johnson, P.A., Beresnev, I.A. and Zeng, Y. (1997), "Nonlinear ground-motion amplification by sediments during the 1994 Northridge earthquake.", *Nature*, **390**, 599-602.

Gelagoti, F., Kourkoulis, R., Anastasopoulos, I., Tazoh, T. and Gazetas, G. (2010), "Seismic wave propagation in a very soft alluvial valley: sensitivity to ground-motion details and soil nonlinearity, and generation of a parasitic vertical component", *Bull. Seismol. Soc. Am.*, **100**(6), 3035-3054. https://doi.org/10.1785/0120100002.

Griffiths, S., Cox, B. and Rathje, E. (2016), "Challenges associated with site response analyses for soft soils subjected to high-intensity input ground motions", *Soil Dyn. Earthq. Eng.*, **85**, 1-10, https://doi.org/10.1016/j.soildyn.2016.03.008.

Iyisan, R. and Khanbabazadeh, H. (2013), "A numerical study on the basin edge effect on soil amplification", *Bull. Earthq. Eng.*, **11**, 1305-1323, https://doi.org/10.1007/s10518-013-9451-6.

Jakka, R.S., Hussain, M.D. and Sharma, M.L. (2015), "Effects on amplification of strong ground motion due to deep soils", *Geomech. Eng.*, **8**(5), 663-674. https://doi.org/10.12989/gae.2015.8.5.663.

Kamalian, M., Jafari, M.K., Sohrabi-Bidar, A., Razmkhah, A. and Gatmiri, B. (2006), "Time domain two-dimensional site response analysis of non-homogeneous topographic structures by a hybrid BE/FE method", *Soil Dyn. Earthq. Eng.*, **26**, 753-765. https://doi.org/10.1016/j.soildyn.2005.12.008.

Kamiyama, M. and Satoh, T. (2002), "Seismic response analysis of laterally inhomogeneous ground with emphasis on strains", *Soil Dyn. Earthq. Eng.*, **22**, 877-884. https://doi.org/10.1016/S0267-7261(02)00110-0.

Khanbabazadeh, H., Hasal, M.E. and Iyisan, R. (2019), "2D seismic response of the Duzce Basin, Turkey", *Soil Dyn. Earthq. Eng.*, **125**, 105754. https://doi.org/10.1016/j.soildyn.2019.105754.

Khanbabazadeh, H. and Iyisan, R. (2014a), "A numerical study on the 2D behavior of clayey basins", *Soil Dyn. Earthq. Eng.*, **66**, 31-41. https://doi.org/10.1016/j.soildyn.2014.06.029.

Khanbabazadeh, H. and Iyisan, R. (2014b), "A numerical study on the 2D behavior of the single and layered clayey basins", *Bull. Earthq. Eng.*, **12**, 1515-1536, https://doi.org/10.1007/s10518-014-9590-4.

Khanbabazadeh, H., Iyisan, R., Ansal, A. and Zulfikar, C. (2018), "Nonlinear dynamic behavior of the basins with 2D bedrock", *Soil Dyn. Earthq. Eng.*, **107**, 108-115, https://doi.org/10.1016/j.soildyn.2018.01.011.

Khanbabazadeh, H., Iyisan, R., Ansal, A. and Hasal, M.E. (2016), "2D non-linear seismic response of the Dinar basin,Turkey", *Soil Dyn. Earthq. Eng.*, **89**, 5-11. https://doi.org/10.1016/j.soildyn.2016.07.021.

Khanbabazadeh, H., Iyisan, R., Ozaslan, B. (2022), "2D seismic response of shallow sandy basins subjected to obliquely incident waves", *Soil Dyn. Earthq. Eng.*, **153**, 107080. Doi.org/10.1016/j.soildyn.2021.107080.

Khanbabazadeh, H., Iyisan, R. and Ozaslan, B. (2022), "Seismic behavior of the shallow clayey basins subjected to obliquely incident wave", *Geomech. Eng.*, **31**(2), 183-195. https://doi.org/10.12989/gae.2022.31.2.183.

Khanbabazadeh, H., Zulfika,r A.C. and Yesilyurt, A. (2020), "Basin edge effect on industrial structures damage pattern at clayeybasins", *Geomech. Eng.*, **23**(6), 575-585. https://doi.org/10.12989/gae.2020.23.6.575.

Khoshghalb, A., Shafee, A., Tootoonchi, A., Ghaffaripour, O. and Jazaeri, S.A. (2020), "Application of the smoothed point interpolation methods in computational geomechanics: A comparative study", *Comput. Geotech*,. **126**, 103714. https://doi.org/10.1016/j.compgeo.2020.103714.

Kozo Keikaku Inc, (1995), "SuperFLUSH/3D Manual".

Lysmer, J. and Kuhlemeyer, R.L. (1969), "Finite dynamic model for infinite media", *J. Eng. Mech*., **95**(4), 859-877.

Makra, K., Chavez-Garcıa, F.J., Raptakis, D. and Pitilakis, K. (2005), "Parametric analysis of the seismic response of a 2D sedimentary valley: implications for code implementations of complex site effects", *Soil Dyn. Earthq. Eng*., **25**, 303-315. https://doi.org/10.1016/j.soildyn.2005.02.003.

Makra, K. and Chavez-Garci, F.J. (2016), "Site effects in 3D basins using 1D and 2D models: an evaluation of the differences based on simulations of the seismic response of Euroseistest", *Bull. Earthq. Eng*., **14**, 1177-1194. https://doi.org/10.1007/s10518-015-9862-7.

Madiai, C., Facciorusso, J. and Gargini, E. (2017), "Numerical modeling of seismic site effects in a shallow alluvial basin of the northern Apennines (Italy)", *Bull. Seismol. Soc. Am.*, **107**, 2094-2105. https://doi.org/10.1785/0120160293.

Madiai, C., Facciorusso, J., Gargini, E. and Baglione, M. (2016), "1D versus 2D site effects from numerical analyses on a cross section at Barberino di Mugello (Tuscany, Italy)", *Procedia Eng.*, **158**, 499-504. https://doi.org/10.1016/j.proeng.2016.08.479.

Manakou, M.V., Raptakis, D.G., Chavez-Garci, F.J., Apostolidis, P.I. and Pitilakis K.D. (2010), "3D soil structure of the Mygdonian basin for site response analysis", *Soil Dyn. Earthq. Eng*., **30**, 1198-1211. https://doi.org/10.1016/j.soildyn.2010.04.027.

Mayoral, J.M., Asimaki, D., Tepalcapa, S., Wood, C., Sancha, A.R., Hutchinson, T., Franke, K. and Montalva, G. (2019), "Site

effects in Mexico City basin: Past and present", *Soil Dyn. Earthq. Eng.*, **121**, 369-382. https://doi.org/10.1016/j.soildyn.2019.02.028.

Nagashima, F., Matsushima, S., Kawase, H., Sánchez-Sesma, F.J., Hayakawa, T., Satoh, T. and Oshima, M. (2014), "Application of horizontal-to-vertical spectral ratios of earthquake ground motions to identify subsurface structures at and around the K-NET site in Tohoku, Japan", *Bull. Seismol. Soc. Am.*, **104**(5), 2288-2302. https://doi.org/10.1785/0120130219.

Ozaslan, B., Iyisan, R., Hasal, M.E., Khanbabazadeh, H. and Yamanaka, H. (2022), "Assessment of the design spectrum with aggravation factors by 2D nonlinear numerical analyses: a case study in the Gemlik Basin, Turkey", *Bull. Earthq. Eng.*, **20**(3), 1371-1395. https://doi.org/10.1007/s10518-021-01296-6.

Pelekis, P., Batilas, A., Pefani, E., Vlachakis, V. and Athanasopoulos, G. (2017), "Surface topography and site stratigraphy effects on the seismic response of a slope in the Achaia-Ilia (Greece) 2008 Mw6.4 earthquake", *Soil Dyn. Earthq. Eng.*, **100**, 538-554. https://doi.org/10.1016/j.soildyn.2017.05.038.

Riga, E., Makra, K. and Pitilakisa, K. (2018), "Investigation of the effects of sediments inhomogeneity and nonlinearity on aggravation factors for sedimentary basins", *Soil Dyn. Earthq. Eng.*, **110**, 284-299. https://doi.org/10.1016/j.soildyn.2018.01.016.

Rodriguez-Plata, R., Ozcebe, A.G., Smerzini, C. and Lai, C.G. (2021), "Aggravation factors for 2D site effects in sedimentary basins: The case of Norcia, central Italy", *Soil Dyn. Earthq. Eng.*, **149**, 106854. https://doi.org/10.1016/j.soildyn.2021.106854.

Rong, M., Wang, Z., Woolery, E.W., Lyu, Y., Li, X. and Li, S. (2016), "Nonlinear site response from the strong ground-motion recordings in western China", *Soil Dyn. Earthq. Eng.*, **82**, 99-110. https://doi.org/10.1016/j.soildyn.2015.12.001.f.

Roy, N. and Sahu, R.B. (2012), "Site specific ground motion simulation and seismic response analysis for microzonation of Kolkata", *Geomech. Eng.*, **4**(1), 1-18. https://doi.org/10.12989/gae.2012.4.1.001.

Saenz, M., Sierra, C., Vergara, J., Jaramillo, J. and Gomez, J. (2019), "Site specific analysis using topography conditioned response spectra", *Soil Dyn. Earthq. Eng.*, **123**, 470-497. https://doi.org/10.1016/j.soildyn.2019.03.004.

Safak, E. (2001), "Local site effects and dynamic soil behavior", *Soil Dyn. Earthq. Eng.,* **21**, 453-458. https://doi.org/10.1016/S0267-7261(01)00021-5.

Saffarian, M.A. and. Bagheripour, M.H. (2014)," Seismic response analysis of layered soils considering effect of surcharge mass using HFTD approach. Part I: basic formulation and linear HFTD", *Geomech. Eng.*, **6**(6), 517-530. https://doi.org/10.12989/gae.2014.6.6.517.

Salehi Dezfooli, M., Khoshghalb, A. and Shafee, A. (2022), "An automatic adaptive edge-based smoothed point interpolation method for coupled flow-deformation analysis of saturated porous media", *Comput. Geotech.*, **145**, 104672. https://doi.org/10.1016/j.compgeo.2022.104672.

Satoh, T., Kawase, H. and Sato, T. (1995) "Nonlinear behavior of soil sediments identified by using borehole records observed at the Ashigaravalley, Japan", *Bull Seismol Soc Am*, **85**:1821–34. https://doi.org/10.1785/BSSA0850061821

Semblat, J.F., Dangla, P., Khama, M. and Duva, A.M. (2002), "Seismic site effects for shallow and deep alluvial basins: In-depth motion and focusing effect", *Soil Dyn. Earthq. Eng.*, **22**, 849-854. https://doi.org/10.1016/S0267-7261(02)00107-0.

Semblat, J.F., Duval, A.M. and Dangla, P. (2000), "Numerical Analysis of Seismic Wave Amplification in Nice (France) and comparisons with experiments", *Soil Dyn. Earthq. Eng.*, **19**(5), 347-362. https://doi.org/10.1016/S0267-7261(00)00016-6.

Shafee, A. and Khoshghalb, A. (2021), "An improved node-based smoothed point interpolation method for coupled hydro-mechanical problems in geomechanics", *Comput. Geotech.*, **139**, 104415. https://doi.org/10.1016/j.compgeo.2021.104415

Shafee, A. and Khoshghalb, A. (2022), "Particle node-based smoothed point interpolation method with stress regularisation for large deformation problems in geomechanics", *Comput. Geotech.*, **141**, 104494. https://doi.org/10.1016/j.compgeo.2021.104494.

Shani-Kadmiel S., Tsesarsky M., Louie J. N., Gvirtzman Z. (2012), "Simulation of seismic-wave propagation through geometrically complex basins: the Dead Sea Basin", *Bull. Seismol. Soc. Am*. **102**(4), 1729-1739. https://doi.org/10.1785/0120110254.

Shiuly, A., Sahu, R.B. and Mandal, S. (2015), "Seismic microzonation of Kolkata", *Geomech. Eng*., **9**(2), 125-144. https://doi.org/10.12989/gae.2015.9.2.125.

Silahtar, A. and Kanbur, M.Z. (2021), "1D nonlinear site response analysis of the Isparta Basin (Southwestern Turkey) with surface wave (ReMi) and borehole data", *Environ. Earth Sci.*, **80**, 268. https://doi.org/10.1007/s12665-021-09551-4.

Sonmezer, Y.B., Bas, S., Isik, N.S. and Akbas, S.O. (2018), "Linear and nonlinear site response analyses to determine dynamic soil properties of Kirikkale", *Geomech. Eng.*, **16**(4), 435-448. DOI:http://dx.doi.org/10.12989/gae.2018.16.4.435

Sonmezer, Y.B. and Celiker, M. (2020), "Determination of seismic hazard and soil response of a critical region in Turkey considering far-field and near-field earthquake effect", *Geomech. Eng.*, **20**(2), 131-146. https://doi.org/10.12989/gae.2020.20.2.131.

Stamati, O., Klimis, N. and Lazaridis, T. (2016), "Evidence of complex site effect sand soil non-linearity numerically estimated by 2D vs 1D seismic response analyses in the city of Xanthi", *Soil Dyn. Earthq. Eng.*, **87**, 101-115. https://doi.org/10.1016/j.soildyn.2016.05.006.

Stanko, D., Gulerce, Z., Markusic, S. and Salic, R. (2019), "Evaluation of the site amplification factors estimated by equivalent linear site response analysis using time series and random vibration theory based approaches", *Soil Dyn. Earthq. Eng.*, **117**, 16-29. https://doi.org/10.1016/j.soildyn.2018.11.007.

Wen, K.L., Chang, T.M. and Lin, C.M. (2006), "Identification of nonlinear site response using the H/V spectral ratiomethod", *Terr. Atmos. Ocean Sci.*, **17**(3), 533-546. https://doi.org/10.3319/TAO.2006.17.3.533(T).

Yniesta, S., Brandenberg, S.J. and Shafiee, A. (2017), "ARCS: A one dimensional nonlinear soil model for ground response analysis", *Soil Dyn. Earthq. Eng.*, **102**, 75-85. https://doi.org/10.1016/j.soildyn.2017.08.015

Zhang. J. and Zhao, J.X. (2009), "Response spectral amplification ratios from 1- and 2 dimensional nonlinear soil site models", *Soil Dyn. Earthq. Eng.*, **29**, 563-573. https://doi.org/10.1016/j.soildyn.2008.06.006.

Zhu, C., Chavez-Garcia, F.J., Thambiratnam, D. and Gallage, C. (2018), "Quantifying the edge-induced seismic aggravation in shallow basins relative to the 1D SH model", *Soil Dyn. Earthq. Eng*., **115**, 402-412. https://doi.org/10.1016/j.soildyn.2018.08.025.

Zhu, C. and Thambiratnam, D. (2016), "Interaction of geometry and mechanical property of trapezoidal sedimentary basins with incident SH waves", *Bull. Earthq. Eng*,, **14**, 2977–3002. https://doi.org/10.1007/s10518-016-9938-z

GC